

# Parallel Finite Element Modeling of Earthquake Ground Response and Liquefaction

Jinchi Lu<sup>1</sup>, Jun Peng<sup>2</sup>, Ahmed Elgamal<sup>3</sup>, Zhaohui Yang<sup>4</sup>, and Kincho H. Law<sup>5</sup>

## Abstract

Parallel computing is a promising approach to alleviate the computational demand in conducting large-scale finite element analyses. This paper presents a numerical modeling approach for earthquake ground response and liquefaction using the parallel nonlinear finite element program, ParCYCLIC, which is designed for distributed-memory message-passing parallel computer systems. In ParCYCLIC, finite elements are employed within an incremental plasticity, coupled solid-fluid formulation framework. A constitutive model calibrated by physical tests represents the salient characteristics of sand liquefaction and associated accumulation of shear deformations. Key elements of the computational strategy employed in ParCYCLIC include the development of a parallel sparse direct solver, the deployment of an automatic domain decomposer, and the use of the Multilevel Nested Dissection algorithm for the ordering of finite element nodes. Simulation results of centrifuge test models using ParCYCLIC are presented. Performance results from grid models and geotechnical simulations show that ParCYCLIC is efficiently scalable to a large number of processors.

**Keywords:** parallel finite element method, domain decomposition, liquefaction, parallel speedup, earthquake, site amplification

---

<sup>1</sup> Ph.D. Candidate, Department of Structural Engineering, University of California, San Diego, CA 92093. E-mail: jinlu@ucsd.edu.

<sup>2</sup> Research Associate, Department of Civil and Environmental Engineering, Stanford University, Stanford, CA 94305. E-mail: junpeng@stanford.edu.

<sup>3</sup> Professor, Department of Structural Engineering, University of California, San Diego, CA 92093. E-mail: elgamal@ucsd.edu.

<sup>4</sup> Research Associate, Department of Structural Engineering, University of California, San Diego, CA 92093. E-mail: zhyang@ucsd.edu.

<sup>5</sup> Professor, Department of Civil and Environmental Engineering, Stanford University, Stanford, CA 94305. E-mail: law@ce.stanford.edu.

## 1. Introduction

Large-scale finite element (FE) simulations of earthquake ground response including liquefaction effects often require a lengthy execution time. This is necessitated by the complex algorithms of coupled solid-fluid formulation, the associated highly nonlinear plasticity-based constitutive models, and the time domain step-by-step earthquake computations. In view of the finite memory size and the limitation of current operating systems (e.g. Linux, MS Windows, and so forth), large-scale earthquake simulations may not be feasible on single-processor computers. Utilization of parallel computers, which combine the resources of multiple processing and memory units, can potentially reduce the solution time significantly and allow simulations of large and complex models that may not fit into a single processing unit.

The concept of parallel computing has been successfully applied to various structural and geotechnical nonlinear finite element problems. Nikishkov et al. (1998) developed a semi-implicit parallel FE code ITAS3D using the domain decomposition method and a direct solver for an IBM SP2 computer. They reported that the parallel implementation could only be efficiently scalable to a moderate number of processors (e.g. 8). Rometo et al. (2002) attempted to perform nonlinear analysis for reinforced concrete three-dimensional frames using different types of parallel computers, including a cluster of personal computers. McKenna (1997) proposed a parallel object-oriented programming framework, which employs a dynamic load balancing scheme to allow element migration between sub-domains in order to optimize CPU usage. Krysl et al (Krysl and Belytschko 1998; Krysl and Bittnar 2001) presented node-cut and element-cut partitioning strategies for the parallelization of explicit finite element dynamics. They found that node-cut partitioning could yield higher parallel efficiency than element-cut partitioning. Bielak et al (1999; 2000) modeled earthquake ground motion in large sedimentary basins using a 3D parallel linear finite element program with an explicit integration procedure. They noted that the implementation of implicit time integration approach is challenging on distributed memory computers, requiring global information exchange (Bao et al. 1998; Hisada et al. 1998; Bielak et al. 1999; Bielak et al. 2000).

The research reported herein focuses on the development of a state-of-the-art nonlinear parallel finite element program for earthquake ground response and liquefaction simulation. The parallel code, ParCYCLIC, is implemented based on a serial program CYCLIC, which is a nonlinear finite element program developed to analyze liquefaction-induced seismic response (Parra 1996; Yang and Elgamal 2002). Extensive calibration of CYCLIC has been conducted with results from experiments and full-scale response of earthquake simulations involving ground liquefaction. In ParCYCLIC, the calibrated serial code for modeling of earthquake geotechnical phenomena is combined with advanced computational methodologies to facilitate the simulation of large-scale systems and broaden the scope of practical applications.

In the following sections, the essential features of the finite element formulation and the constitutive model employed in ParCYCLIC are described. Thereafter, details on the implementation of ParCYCLIC are presented, followed by numerical simulations of centrifuge seismic site response experiments using ParCYCLIC. The parallel performance of ParCYCLIC is then discussed.

## **2. Finite element formulation**

In CYCLIC and ParCYCLIC, the saturated soil system is modeled as a two-phase material based on the Biot (1962) theory for porous media. A numerical framework of this theory, known as  $u-p$  formulation, was implemented (Parra 1996; Yang 2000; Yang and Elgamal 2002). In the  $u-p$  formulation, displacement of the soil skeleton  $u$ , and pore pressure  $p$ , are the primary unknowns (Chan 1988; Zienkiewicz et al. 1990). The implementation of CYCLIC is based on the following assumptions: small deformation and rotation, constant density of the solid and fluid in both time and space, locally homogeneous porosity which is constant with time, incompressibility of the soil grains, and equal accelerations for the solid and fluid phases.

The  $u-p$  formulation as defined by Chan (1988) consists of: i) equation of motion for the solid-fluid mixture, and ii) equation of mass conservation for the fluid phase, incorporating equation of motion for the fluid phase and Darcy's law. These two governing equations can be expressed in the finite element matrix form as follows (Chan 1988):

$$\mathbf{M}\ddot{\mathbf{U}} + \int_{\Omega} \mathbf{B}^T \boldsymbol{\sigma}' d\Omega + \mathbf{Q}\mathbf{p} - \mathbf{f}^s = \mathbf{0} \quad (1a)$$

$$\mathbf{Q}^T \dot{\mathbf{U}} + \mathbf{S}\dot{\mathbf{p}} + \mathbf{H}\mathbf{p} - \mathbf{f}^p = \mathbf{0} \quad (1b)$$

where  $\mathbf{M}$  is the mass matrix,  $\mathbf{U}$  the displacement vector,  $\mathbf{B}$  the strain-displacement matrix,  $\boldsymbol{\sigma}'$  the effective stress tensor (determined by the soil constitutive model described below),  $\mathbf{Q}$  the discrete gradient operator coupling the solid and fluid phases,  $\mathbf{p}$  the pore pressure vector,  $\mathbf{S}$  the compressibility matrix, and  $\mathbf{H}$  the permeability matrix. The vectors  $\mathbf{f}^s$  and  $\mathbf{f}^p$  represent the effects of body forces and prescribed boundary conditions for the solid-fluid mixture and the fluid phase respectively.

In eq. 1a (equation of motion), the first term represents inertia force of the solid-fluid mixture, followed by internal force due to soil skeleton deformation, and internal force induced by pore-fluid pressure. In eq. 1b (equation of mass conservation), the first two terms represent the rate of volume change for the soil skeleton and the fluid phase respectively, followed by the seepage rate of the pore fluid. Eqs. 1a and 1b are integrated in the time space using a single-step predictor multi-corrector scheme of the Newmark type (Chan 1988; Parra et al. 1996). In the current implementation, the solution is obtained for each time step using the modified Newton-Raphson approach (Parra 1996).

### 3. Soil constitutive model

The second term in eq. 1a is defined by the soil stress-strain constitutive model. The finite element program incorporates a soil constitutive model (Parra 1996; Yang and Elgamal 2002; Elgamal et al. 2003; Yang et al. 2003) based on the original multi-surface-plasticity theory for frictional cohesionless soils (Prevost 1985). This model was developed with emphasis on simulating the liquefaction-induced shear strain accumulation mechanism in clean medium-dense sands (Elgamal et al. 2002a; Elgamal et al. 2002b; Yang and Elgamal 2002; Elgamal et al. 2003; Yang et al. 2003). Special attention was given to the deviatoric-volumetric strain coupling (dilatancy) under cyclic loading, which causes increased shear stiffness and strength at large cyclic shear strain excursions (i.e., cyclic mobility).

The constitutive equation is written in incremental form as follows (Prevost 1985):

$$\dot{\boldsymbol{\sigma}}' = \mathbf{E} : (\dot{\boldsymbol{\varepsilon}} - \dot{\boldsymbol{\varepsilon}}^p) \quad (2)$$

where  $\dot{\boldsymbol{\sigma}}'$  is the rate of effective Cauchy stress tensor,  $\dot{\boldsymbol{\epsilon}}$  the rate of deformation tensor,  $\dot{\boldsymbol{\epsilon}}^p$  the plastic rate of deformation tensor, and  $\mathbf{E}$  the isotropic fourth-order tensor of elastic coefficients. The rate of plastic deformation tensor is defined by:  $\dot{\boldsymbol{\epsilon}}^p = \mathbf{P} \langle L \rangle$ , where  $\mathbf{P}$  is a symmetric second-order tensor defining the direction of plastic deformation in stress space,  $L$  the plastic loading function, and the symbol  $\langle \rangle$  denotes the McCauley's brackets (i.e.,  $\langle L \rangle = \max(L, 0)$ ). The loading function  $L$  is defined as:  $L = \mathbf{Q} : \dot{\boldsymbol{\sigma}}' / H'$  where  $H'$  is the plastic modulus, and  $\mathbf{Q}$  a unit symmetric second-order tensor defining yield-surface normal at the stress point (i.e.,  $\mathbf{Q} = \nabla f / \|\nabla f\|$ ), with the yield function  $f$  selected of the following form (Elgamal et al. 2003):

$$f = \frac{3}{2} (s - (p' + p'_0) \boldsymbol{\alpha}) : (s - (p' + p'_0) \boldsymbol{\alpha}) - M^2 (p' + p'_0)^2 = 0 \quad (3)$$

in the domain of  $p' \geq 0$ . The yield surfaces in principal stress space and deviatoric plane are shown in Fig. 1. In eq. 3,  $s = \boldsymbol{\sigma}' - p' \boldsymbol{\delta}$  is the deviatoric stress tensor,  $p'$  the mean effective stress,  $p'_0$  a small positive constant (1.0 kPa in this paper) such that the yield surface size remains finite at  $p' = 0$  for numerical convenience (Fig. 1),  $\boldsymbol{\alpha}$  a second-order kinematic deviatoric tensor defining the surface coordinates, and  $M$  dictates the surface size. In the context of multi-surface plasticity, a number of similar surfaces with a common apex form the hardening zone (Fig. 1). Each surface is associated with a constant plastic modulus. Conventionally, the low-strain (elastic) module and plastic module are postulated to increase in proportion to the square root of  $p'$  (Prevost 1985).

The flow rule is chosen so that the deviatoric component of flow  $\mathbf{P}' = \mathbf{Q}'$  (associative flow rule in the deviatoric plane), and the volumetric component  $\mathbf{P}''$  defines the desired amount of dilation or contraction in accordance with experimental observations. Consequently,  $\mathbf{P}''$  defines the degree of non-associativity of the flow rule and is given by (Parra 1996):

$$\mathbf{P}'' = \frac{(\eta/\bar{\eta})^2 - 1}{(\eta/\bar{\eta})^2 + 1} \boldsymbol{\psi} \quad (4)$$

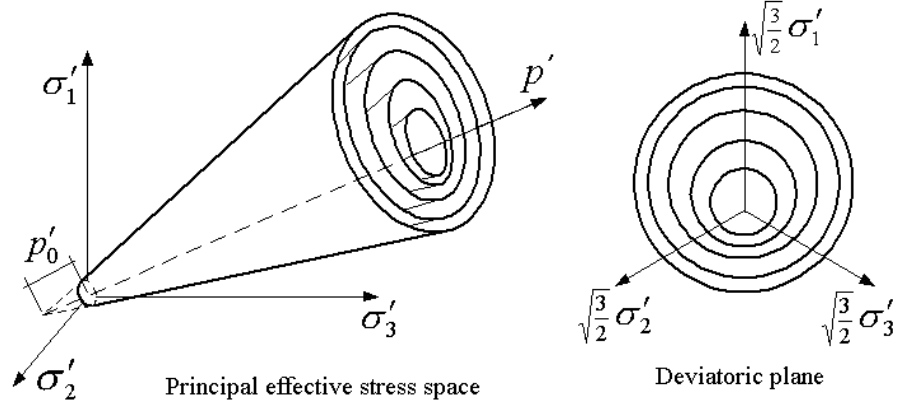


Figure 1: Conical yield surfaces for granular soils in principal stress space and deviatoric plane (Prevost 1985; Lacy 1986; Parra et al. 1996; Yang 2000)

where  $\eta = ((3/2)s : s)^{1/2} / p'$  is effective stress ratio,  $\bar{\eta}$  a material parameter defining the stress ratio along the phase transformation (PT) surface (Ishihara et al. 1975), and  $\Psi$  a scalar function controlling the amount of dilation or contraction depending on the level of confinement and/or cumulated plastic deformation (Elgamal et al. 2003). The sign of  $(\eta / \bar{\eta})^2 - 1$  dictates dilation or contraction. If the sign is negative, the stress point lies below the PT surface and contraction takes place (phase 0-1, Fig. 2). On the other hand, the stress point lies above the PT surface when the sign is positive and dilation occurs under shear loading (phase 2-3, Fig. 2). At low confinement levels, accumulation of plastic deformation may be prescribed (phase 1-2, Fig. 2) before the onset of dilation (Elgamal et al. 2003).

A purely deviatoric kinematic hardening rule is chosen according to (Prevost 1985):

$$p' \dot{\alpha} = b \boldsymbol{\mu} \quad (5)$$

where  $\boldsymbol{\mu}$  is a deviatoric tensor defining the direction of translation and  $b$  is a scalar magnitude dictated by the consistency condition. In order to enhance computational efficiency, the direction of translation  $\boldsymbol{\mu}$  is defined by a new rule (Parra 1996; Elgamal et al. 2003), which maintains the original concept of conjugate-points contact by Mroz (Mroz 1967). Thus, all yield surfaces may translate in stress space within the failure envelope.

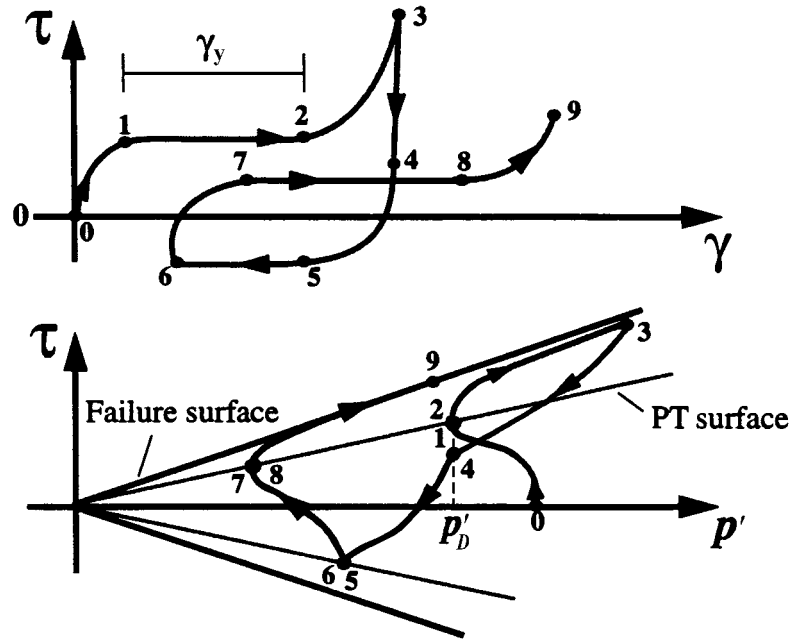


Figure 2: Shear stress-strain and effective stress path under undrained shear loading conditions (Parra 1996; Yang 2000)

The employed model has been extensively calibrated for clean Nevada Sand at  $D_r \approx 40\%$  (Parra 1996; Yang 2000). Calibration was based on results of monotonic and cyclic laboratory tests (Arulmoli et al. 1992, fig 3), as well as data from level-ground and mildly inclined infinite-slope dynamic centrifuge-model simulations (Dobry et al. 1995; Taboada 1995). The main modeling parameters include (Table 1) standard dynamic soil properties such as low-strain shear modulus and friction angle, as well as calibration constants to control the dilatancy effects (phase transformation angle, contraction and dilation parameters), and the level of liquefaction-induced yield strain ( $\gamma_y$ ).

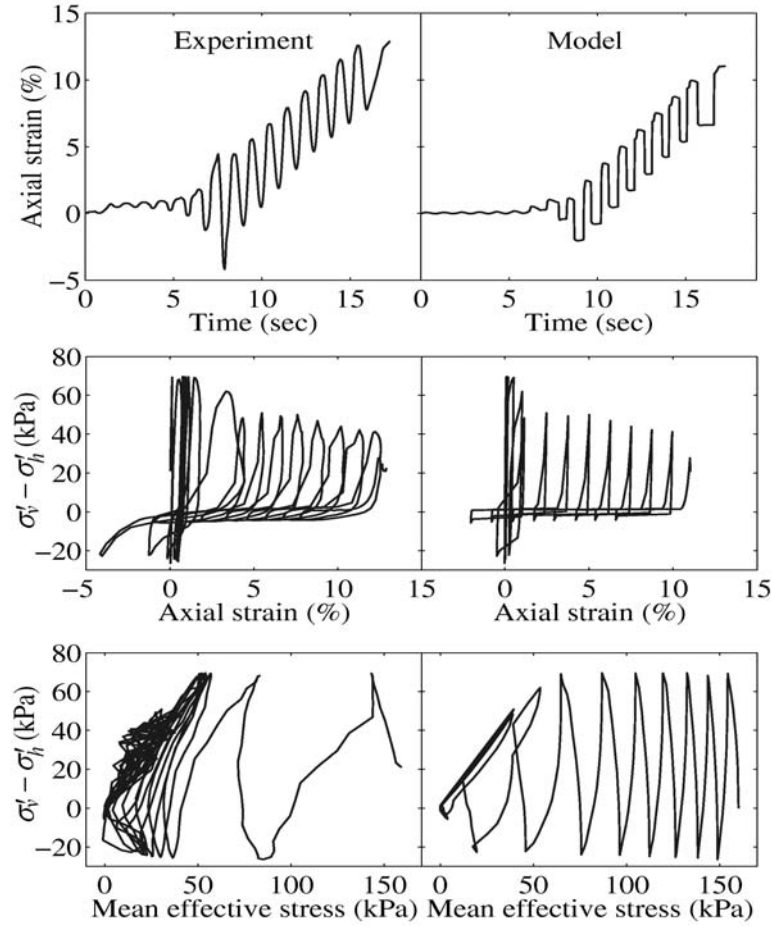


Figure 3: Recorded and computed results of anisotropically consolidated, undrained cyclic triaxial test (Nevada Sand at 40% relative density) with static shear stress bias (Arulmoli et al. 1992; Yang 2000)

Table 1: Model parameters calibrated for  $D_r = 40\%$  Nevada Sand (Elgamal et al. 2002b)

Main calibration experiment	Parameter	Value
Drained monotonic tests	Low-strain shear modulus $G_r$ (at 80 kPa mean effective confinement)	33.3 MPa
	Friction angle $\phi$	31.4 degrees
Undrained cyclic test	Liquefaction yield strain $\gamma_y$ (Fig. 2, phase 1-2)	1.0 %
RPI Centrifuge Model 1	Contraction parameter $c_1$	0.17
	Contraction parameter $c_2$ (Fig. 2, phase 0-1)	0.05
RPI Centrifuge Model 2	Phase transformation angle $\phi_{PT}$	26.5 degrees
	Dilation parameter $d_1$	0.4
	Dilation parameter $d_2$ (Fig. 2, phase 2-3)	100.0



## **4. Parallel implementation**

### **4.1. Parallel program strategies**

Programming architectures required to take advantage of parallel computers are significantly different from the traditional paradigm for a serial program (Mackay 1992; Law 1994; Suarjana 1994; Aluru 1995; Herndon et al. 1995a; McKenna 1997). In a parallel computing environment, care must be taken to maintain all participating processors busy performing useful computations and to minimize communication among the processors. ParCYCLIC employs the single-program-multiple-data (SPMD) paradigm, a common approach in developing application software for distributed memory parallel computers. In this approach, problems are decomposed using well-known domain decomposition techniques. Each processor of the parallel machine solves a partitioned domain and data communications among sub-domains are performed through message passing. The domain decomposition method (DDM) is attractive in finite element computations on parallel computers because it allows individual sub-domain operations to be performed concurrently on separate processors. The SPMD model has been applied successfully in the development of many parallel finite element programs from legacy serial code (Aluru 1995; Herndon et al. 1995b; De Santiago and Law 1996).

### **4.2. Computational procedures**

The computational procedure of ParCYCLIC is illustrated in Fig. 4. The procedure can be divided into three distinct phases: the initialization phase, the nonlinear solution phase, and the output and postprocessing phase. The initialization phase consists of reading input files, performing mesh partitioning and symbolic factorization. METIS (Karypis and Kumar 1997), which is a set of libraries for graph partitioning developed at the University of Minnesota, is used to partition the finite element mesh at this phase. Specifically, the multilevel nested dissection algorithm in METIS is employed to partition the finite element mesh. An automatic domain decomposer for performing domain decomposition, based on the METIS ordering, is also implemented in ParCYCLIC.

The symbolic factorization is performed after the initialization phase to determine the nonzero pattern of the matrix factor. The storage space for the matrix factor  $L$  is also allocated during the symbolic factorization. Since all the processors need to know the nonzero pattern of the global stiffness

matrix and symbolic factorization generally only takes a small portion of the total runtime, the domain decomposition and symbolic factorization are performed within each processor based on the global input data.

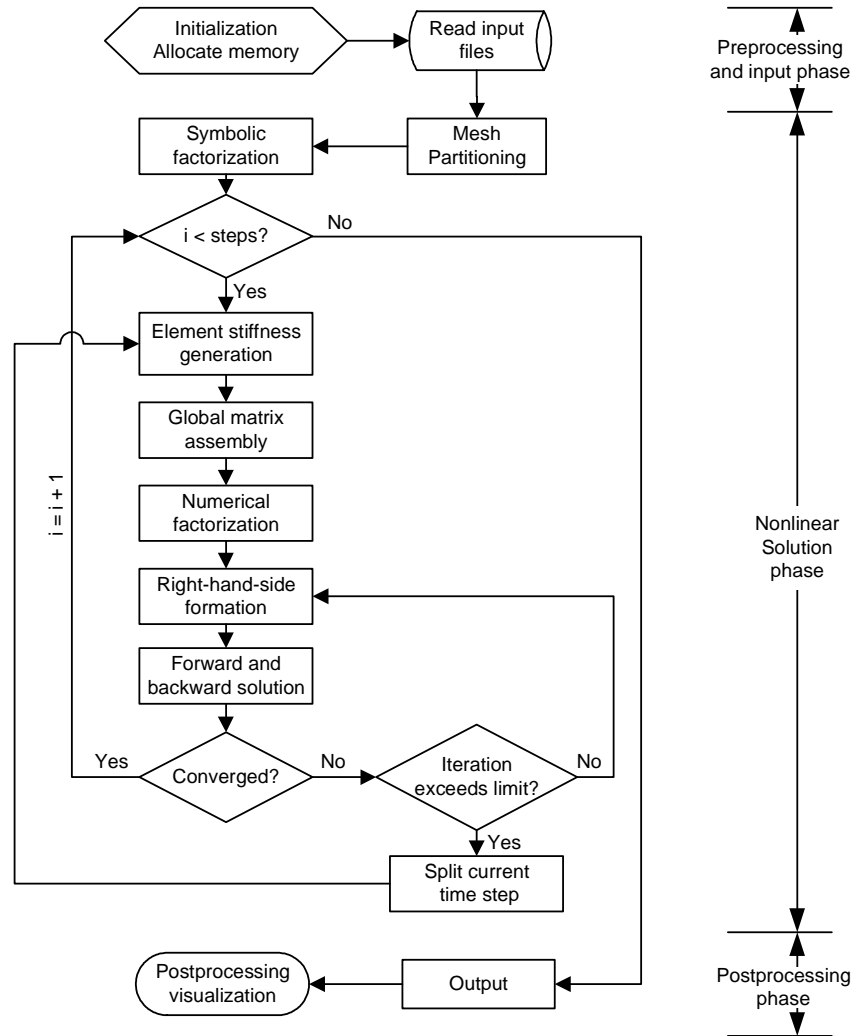


Figure 4. Flowchart of computational procedures in ParCYCLIC

In the nonlinear analysis solution phase, the program essentially goes through a while loop until the number of increments reaches the pre-set limit. In the nonlinear solution phase, the modified Newton-Raphson algorithm is employed, that is, the stiffness matrix at each iteration step uses the same tangential stiffness from the initial step of the increment. The convergence test is performed at the end of each iteration step. If the solution is not converged after a certain number of iterations (e.g., 10 iterations) within a particular time step, the time step will be divided into two steps to expedite

convergence. If the new step still does not converge after a certain number of iterations, then further time step splitting will automatically take place, until convergence is achieved.

The final phase, output and postprocessing, consists of collecting the calculated node response quantities (e.g. displacements, acceleration, pore pressure, and etc.) and element output (includes normal stress, normal strain, volume strain, shear strain, mean effective stress, and etc.) from the different processors. The response quantities and timing results are then written into files for future processing and visualization.

### 4.3. Parallel sparse solver

Nonlinear finite element computations of earthquake simulations involve the iterative solution of sparse symmetric systems of linear equations. Solving the linear system is often the most computational intensive task of a finite element program, especially when an implicit time integration scheme is employed. ParCYCLIC employs a direct sparse solution method proposed and developed by Mackay and Law (1993). The parallel sparse solver is based on a row-oriented storage scheme that takes full advantage of the sparsity of the stiffness matrix. A direct solver is preferred in ParCYCLIC over an iterative solver because even the best-known iterative solver (e.g. the Polynomial Preconditioned Conjugate Gradient method (PPCG)) may exhibit instabilities under certain conditions. For instance, in a nonlinear analysis, an iterative solver may diverge (Romero et al. 2002). The direct solution method is a more stable approach to achieve solution convergence. The concept of the sparse solver incorporated in ParCYCLIC is briefly described below.

Given a linear system of equations  $Kx = f$ , the symmetric sparse matrix  $K$  is often factored into the matrix product  $LDL^T$ , where  $L$  is a lower triangular matrix and  $D$  is a diagonal matrix. The solution vector  $x$  is then computed by a forward solution,  $Lz = f$  or  $z = L^{-1}f$ , followed by a backward substitution  $DL^T x = z$  or  $x = L^{-T}D^{-1}z$ . Sparse matrix factorization can be divided into two phases: symbolic factorization and numeric factorization (Law and Mackay 1993). Symbolic factorization determines the structure of matrix factor  $L$  from that of  $K$  (i.e. locations of nonzero entries). Numeric factorization then

makes use of the data structure determined to compute the numeric values of  $L$  and  $D$ . The nonzero entries in  $L$  can be determined by the original nonzero entries of  $K$  and a list vector, which is defined as:

$$PARENT(j) = \min\{i \mid L_{ij} \neq 0\} \quad (4)$$

in which  $j$  is the column number and  $i$  the row subscript. The array  $PARENT$  represents the row subscript of the first nonzero entry in each column of the lower matrix factor  $L$ . The definition of the array  $PARENT$  results in a monotonically ordered elimination tree  $T$  of which each node has its numbering higher than its descendants (Schreiber 1982; Fenves and Law 1986; Liu 1986, 1988; Mackay et al. 1991). The list array  $PARENT$  contains sufficient information for determining the nonzero structure of any row in  $L$ . Furthermore, by topologically postordering the elimination tree, the nodes in any subtree can be numbered consecutively (Liu 1986). The resulting sparse matrix factor is partitioned into block submatrices where the columns/rows of each block correspond to the node set of a branch in  $T$ . Fig. 5 shows a simple finite element grid and its post-ordered elimination tree representation.

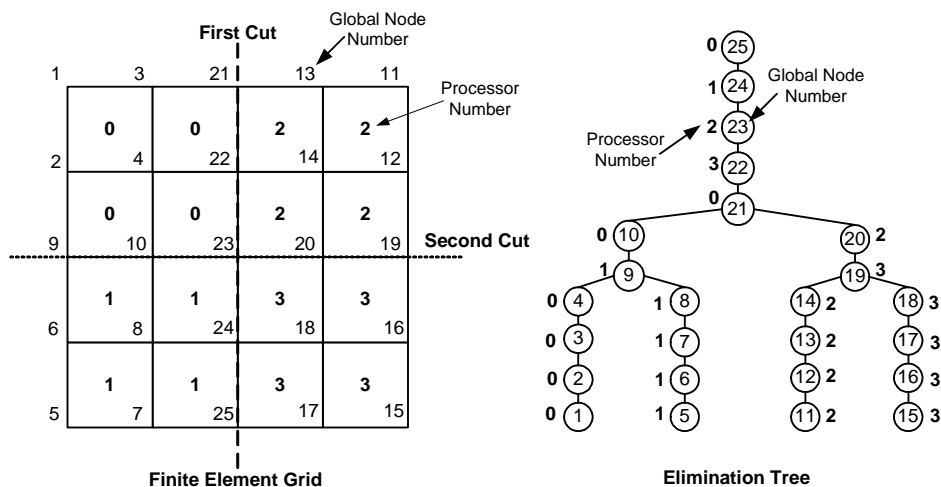


Figure 5: A finite element mesh and its elimination tree representation

For parallel implementation of the sparse matrix factorization, the processor assignment strategy can be based on matrix partitioning according to the post-ordered elimination tree. The coefficients of a sparse matrix factor are distributively stored among the processors according to the column blocks. Essentially, the strategy is to assign the rows corresponding to the nodes along each branch (column block) of the elimination tree to a processor or a group of processors. Beginning at the root of the

elimination tree, the nodes belonging to this branch of the tree are assigned among the available processors in a rotating round robin fashion (Mackay 1992) or a block wrap mapping (Golub and Van Loan 1989). As we traverse down the elimination tree, at each fork of the elimination tree, the group of processors is divided to match the number and the size of the subtrees below the current branch. A separate group of processors is assigned to each branch at the fork and the process is repeated for each subtree.

The parallel numerical factorization procedure is divided into two phases (Law and Mackay 1993). In the first phase, each processor independently factorizes certain portions of the matrix that assigned to a single processor. In the second phase, other portions of the matrix shared by more than one processor are factored. Following the parallel factorization, the parallel forward and backward solution phases proceed to compute the solution to the global system of equations.

## **5. Parallel performance**

ParCYCLIC has been successfully ported on many different types of parallel computers and workstation clusters, including IBM SP machines, SUN super computers, and Linux workstation clusters. To demonstrate the parallel performance of ParCYCLIC, the following shows the performance of ParCYCLIC on the Blue Horizon machine at San Diego Supercomputer Center (NPACI 2003). Blue Horizon is an IBM Scalable POWERparallel (SP) machine with 144 compute nodes, each with eight POWER3 RISC-based processors and with 4 GBytes of memory. Each processor on the node has equal shared access to the memory. The performance of ParCYCLIC is evaluated by using two-dimensional (2D) and three-dimensional (3D) grid models as well as 3D geotechnical finite element models. All timing results mentioned below are collected with nonlinear analysis conducted for one time step (unless stated otherwise).

### **5.1. Solution of finite element grid models**

The first experiment deals with the solution of a number of 2D plane strain finite element grid models of sizes ranging from 150x150 to 300x300 elements, as well as 3D grid models of sizes ranging from 20x20x20 to 35x35x35 elements. The multilevel nested dissection (Karypis and Kumar 1997) for

the grid problems is able to generate a very well-balanced workload distribution for running on a parallel computer. Each processor is responsible for approximately the same number of elements and equations. When there is good load balance, each processor will complete its tasks at about the same time and synchronization costs will be minimized. Table 2 summarizes the execution times of the solution phase for these 2D and 3D grid models for one time step. Excellent parallel speedup is achieved for these grid models up to a certain number of processors, as shown in Table 3. However, the speedup tends to saturate or peak at a certain limit and the performance does not continue to improve with increasing number of processors. This is due to the increased communication overhead as the number of processors continues to increase. It may be noted that some of the grid models, e.g. the 30x30x30 mesh and the 35x35x35 mesh, are too large to fit into the memory of a low number of processors. The execution time for these situations is denoted as N/A in Table 3.

## **5.2. Solution of 3D geotechnical finite element models**

This section presents the results of simulating geotechnical models including a soil-pile interaction model and a stone column centrifuge test model. The soil-pile interaction model shown in Fig. 6 is used to study the loads on a pile group subjected to earthquake-induced liquefaction and lateral spreading. A total of 29,120 3D brick element constitute the FE mesh (Fig. 6). In this soil-pile interaction model, a 3x3 pile group, is embedded in a submerged mild infinite ground slope and subjected to strong base shaking. A three-layer soil profile is used in this model, with a nonliquefiable stratum placed below and above the liquefiable sand. As shown in Fig. 6, a half mesh configuration is used due to geometrical symmetry.

Table 2. Execution times of solution phase for finite element grid models (time in seconds)

Number of processors	2D grid models				3D grid models			
	150x150 <sup>1</sup>	200x200 <sup>2</sup>	250x250 <sup>3</sup>	300x300 <sup>4</sup>	20x20x20 <sup>5</sup>	25x25x25 <sup>6</sup>	30x30x30 <sup>7</sup>	35x35x35 <sup>8</sup>
1	19.66	46.11	98.14	185.70	188.00	674.60	N/A	N/A
2	9.34	19.83	37.60	66.38	93.97	357.00	1016.78	N/A
4	4.57	9.73	17.70	28.68	47.26	187.10	492.82	1359.26
8	2.69	5.56	9.78	16.16	25.59	96.16	248.53	714.91
16	1.81	3.49	5.81	9.22	16.74	54.72	132.73	365.88
32	1.52	2.55	4.05	6.17	12.52	35.14	76.85	188.32
64	2.36	3.60	7.02	6.84	14.80	34.70	58.98	127.23
<sup>1</sup> 68,403 equations; 7,457,460 non-zeros					<sup>5</sup> 37,044 equations; 27,214,674 non-zeros			
<sup>2</sup> 121,203 equations; 14,189,580 non-zeros					<sup>6</sup> 70,304 equations; 66,365,120 non-zeros			
<sup>3</sup> 189,003 equations; 23,724,231 non-zeros					<sup>7</sup> 119,164 equations; 138,930,582 non-zeros			
<sup>4</sup> 271,803 equations; 35,706,300 non-zeros					<sup>8</sup> 186,624 equations; 258,680,240 non-zeros			

Table 3: Speedup factors of the solution phase for finite element grid models

Number of processors	2D grid models				3D grid models			
	150x150	200x200	250x250	300x300	20x20x20	25x25x25	30x30x30 <sup>1</sup>	35x35x35 <sup>2</sup>
1	--	--	--	--	--	--	--	--
2	2.10	2.33	2.61	2.80	2.00	1.89	--	--
4	4.30	4.74	5.54	6.47	3.98	3.61	2.06	--
8	7.31	8.29	10.03	11.49	7.35	7.02	4.09	1.90
16	10.86	13.21	16.89	20.14	11.23	12.33	7.66	3.72
32	12.93	18.08	24.23	30.10	15.02	19.20	13.23	7.22
64	8.33	12.81	13.98	27.15	12.70	19.44	17.24	10.68
<sup>1</sup> Relative to 2 processors								
<sup>2</sup> Relative to 4 processors								

Table 4 summarizes the timing results of the nonlinear analysis for one time step. Note that the results for one processor are not available because the model is too large to fit into the memory of a single processor. The parallel speedup (relative to 2 processors) and the execution times of the solution phase are illustrated in Fig. 7. In a typical earthquake simulation where hundreds or even thousands of time steps may be performed, the solution phase actually dominates, and thus the reported speedup essentially represents that of the entire seismic analysis phase. The performance results demonstrate excellent parallel speedup up to 64 processors for this model.

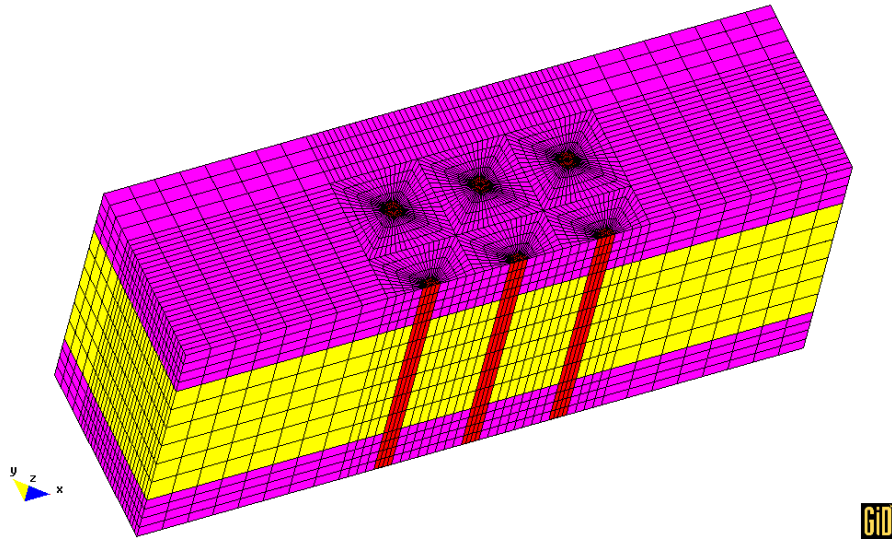


Figure 6: A soil-pile interaction finite element model

Table 4. Solution times for the soil-pile interaction model (time in seconds)

Number of processors	LDL <sup>T</sup> factorization	Forward and backward solve	Solution phase	Total execution time
(130,020 equations; 29,120 elements; 96,845,738 non-zeros in factor L)				
2	332.67	1.41	370.42	455.91
4	166.81	0.78	187.72	286.97
8	85.20	0.45	97.71	186.67
16	50.73	0.29	59.39	147.55
32	27.80	0.23	34.61	124.30
64	18.41	0.26	24.40	116.21
128	18.47	0.83	25.95	124.40

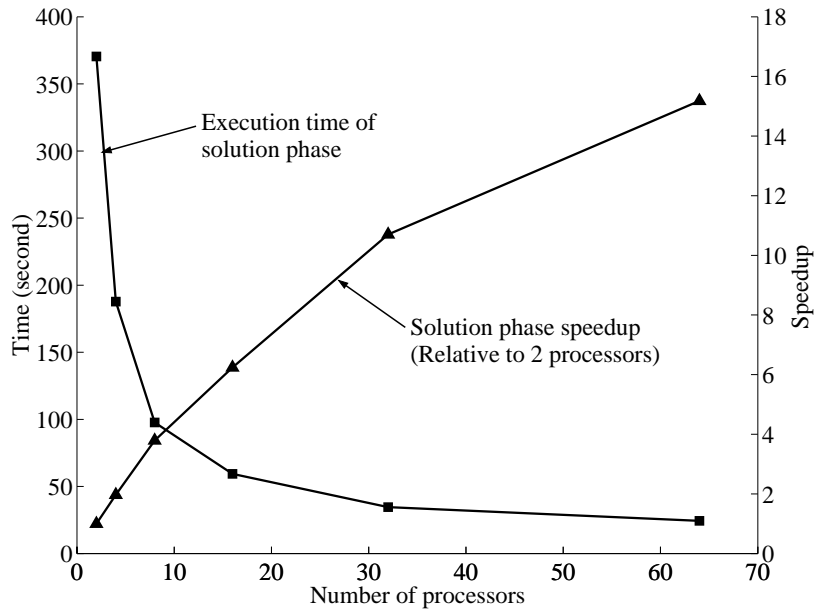


Figure 7. Execution times and speedup of the solution phase for the soil-pile interaction model



Another example is the solution of a stone column centrifuge test model, as shown in Fig. 8. The stone column technique is a ground improvement process where vertical columns of compacted aggregate are installed through the soils to be improved. A series of centrifuge tests were conducted at Rensselaer Polytechnic Institute to assess the performance of this ground improvement method (Adalier et al. 2003). Fig. 8 shows one of the centrifuge test models used in the analysis. In this stone column model, a number of gravel columns are embedded into a fully-saturated silt soil stratum. The model is then subjected to earthquake excitation along the x-direction at the base. Again, a half mesh configuration is used due to geometrical symmetry.

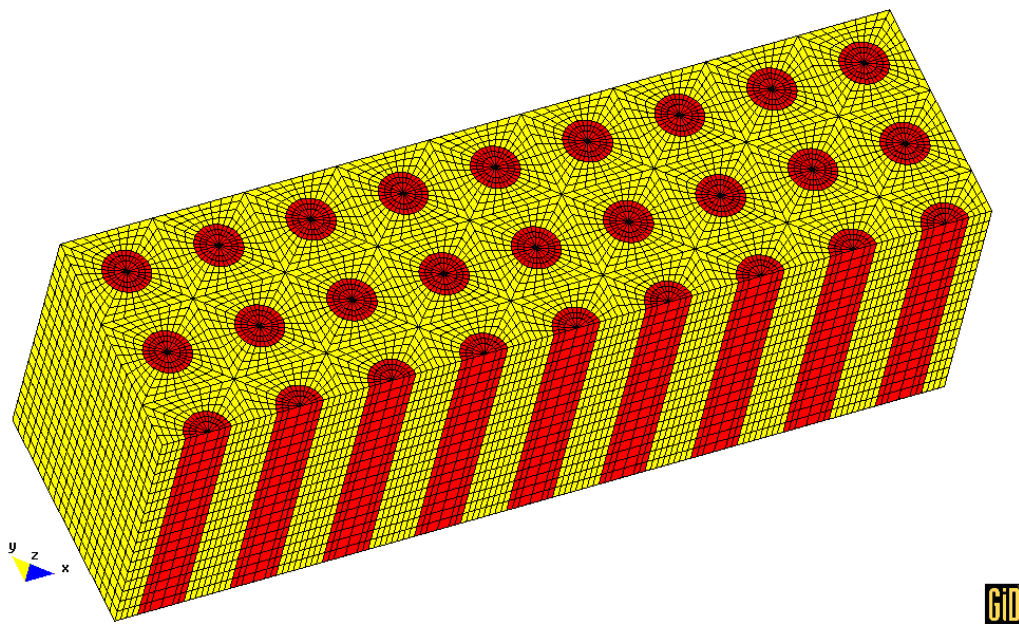


Figure 8. Finite element model of a stone column centrifuge test

Table 5 summarizes the timing results of the solution phase, the  $LDL^T$  numerical factorization and the forward and backward solve, as well as the total execution time for one time step. The speedup and the execution times for the solution phase are illustrated in Fig. 9. Note that the stone column model, with a scale of 364,800 degrees of freedom (dofs), cannot fit into the memory of less than 4 processors. As shown in Table 5 and Fig. 9, excellent parallel speedup is achieved for this model.

Table 5. Solution times for the stone column centrifuge test model (time in seconds)

Number of processors	LDL <sup>T</sup> factorization	Forward and backward solve	Solution phase	Total execution time
(364,800 equations; 84240 elements; 340,514,320 non-zeros in factor <i>L</i> )				
4	1246.08	2.76	1306.87	1769.00
8	665.66	1.56	702.09	1150.17
16	354.99	0.98	378.35	841.38
32	208.90	0.67	225.93	668.02
64	125.05	0.66	142.33	583.98

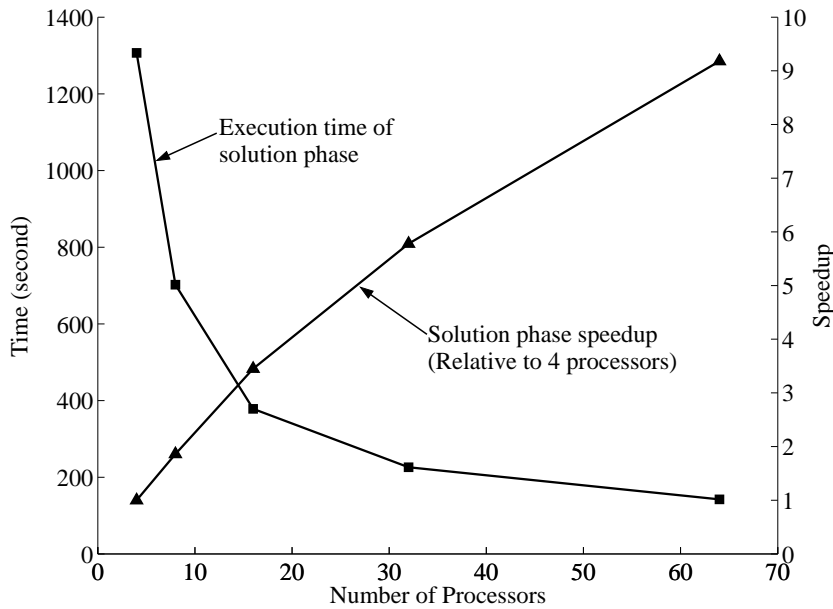


Figure 9. Execution times and speedup of the solution phase for the stone column centrifuge test model

## 6. Numerical simulation of centrifuge experiments

In this section, numerical simulations of centrifuge test models using ParCYCLIC are presented. Two centrifuge model tests (Fig. 10) were conducted by Dobry and Taboada (1994) to simulate the dynamic response of level and mildly sloping sand sites. The employed centrifuge models are (Taboada 1995): VELACS (VERification of Liquefaction Analysis by Centrifuge Studies) Model 1 represents a level site, subjected to a predominantly 2 Hz harmonic base excitation; and VELACS Model 2 represents a mildly inclined infinite slope with an inclination angle of  $2^\circ$ , subjected to a predominantly 2 Hz harmonic base excitation.

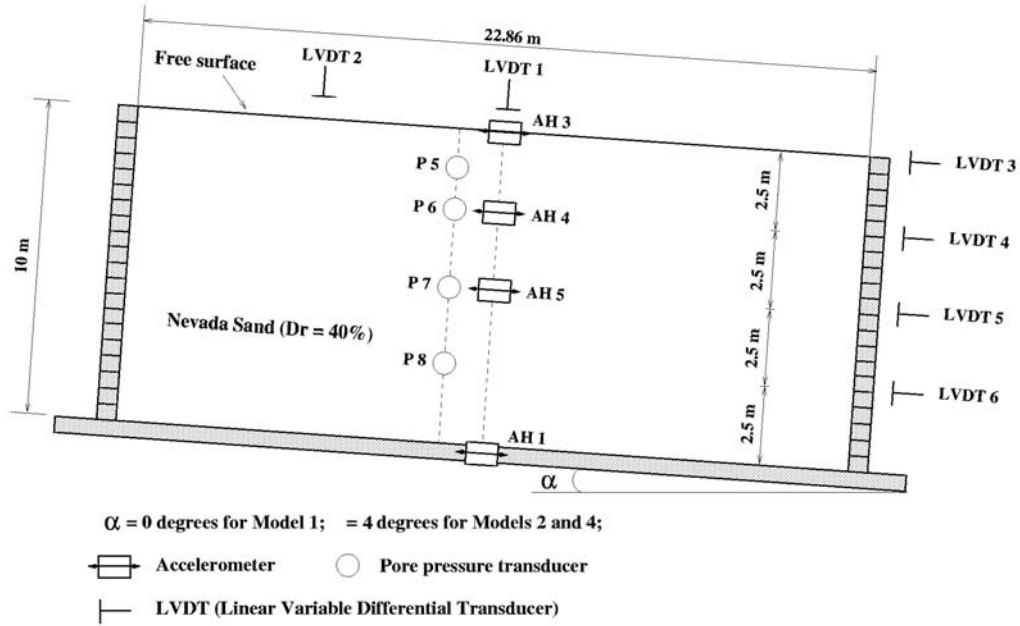


Figure 10: General configurations of RPI models 1 and 2 in laminar container

These tests were performed in a laminated container that allows relative slip between laminates in order to simulate approximately one-dimensional (1D) shear response. Nevada sand was used at  $D_r$  in the range of 40-45%. The soil models were spun to a 50g gravitational field (Taboada 1995). At this gravitational field, the centrifuge models aim to simulate a prototype stratum of 22.86m long, 12.70m wide and 10m high. Water was used as the pore fluid, resulting in a prototype soil permeability equal to 50 times that of the model soil (Tan and Scott 1985).

As mentioned in Section 3, these VELACS centrifuge test models were employed for calibrating CYCLIC (Elgamal et al. 2002b). The simulations performed herein using ParCYCLIC could be viewed as a further calibration procedure with a highly refined 3D finite element mesh. The calibrated main modeling parameters, as shown in Table 1, have been employed in the following 3D simulations.

### 6.1. Numerical modeling

A grid mesh with 60 by 30 by 16 elements (128,588 degrees of freedom in total) was used for the simulations. The boundary conditions were: (i) dynamic excitation was defined as the recorded base acceleration, (ii) at any given depth, displacement degrees of freedom of the downslope and upslope

boundaries were tied together (both horizontally and vertically using the penalty method) to reproduce a 1D shear beam effect (Parra 1996), (iii) the soil surface was traction free, with zero prescribed pore pressure, and (iv) the base and lateral boundaries were impervious. A static application of gravity (model own weight) was performed before seismic excitation. The resulting fluid hydrostatic pressures and soil stress-states served as initial conditions for the subsequent dynamic analysis.

The simulations were conducted using 32 processors on the Blue Horizon machine at San Diego Supercomputer Center (SDSC). The total execution time was approximately 5 hours for the Model 1 simulation and 7 hours for the Model 2 simulation. Note that these simulations cannot fit into a single processor unit due to the limitation of memory size.

## 6.2. Computation results

Figs. 11 and 12 display the computed and recorded lateral accelerations and pore-pressures for Model 1, and Figs. 13 and 14 for Model 2. In general, good agreement is achieved between the computed and the recorded responses. In Model 1, accelerations virtually disappeared at the free surface after about 4 seconds due to liquefaction, as shown in Fig. 11. Liquefaction was reached down to a depth of 5.0m, as indicated by the pore-pressure ratio  $r_u$  approaching 1.0 (dashed lines in Fig. 12,  $r_u = u_e/\sigma_v$  where  $u_e$  is excess pore pressure, and  $\sigma_v$  initial effective vertical stress).

The 2° inclination of Model 2 imposed a static shear stress component (due to gravity), causing accumulated cycle-by-cycle lateral deformation. Despite the relatively mild inclination, all response characteristics (Figs. 13 and 14) are much different from those of Model 1 (Figs. 11 and 12). Surface accelerations were sustained throughout the shaking phase (Fig. 13), and lateral displacement reached a permanent value of 0.4m (Fig. 15). The recorded and computed excess pore pressure histories (Fig. 14) both displayed a number of instantaneous sharp pore pressure drops after initial liquefaction. These drops coincided with the observed and computed acceleration spikes that occurred exclusively in the negative direction (Fig. 13).

As illustrated in Fig. 16, the 3D simulations show that the centrifuge test models behave approximately as a 1D shear beam, as expected.

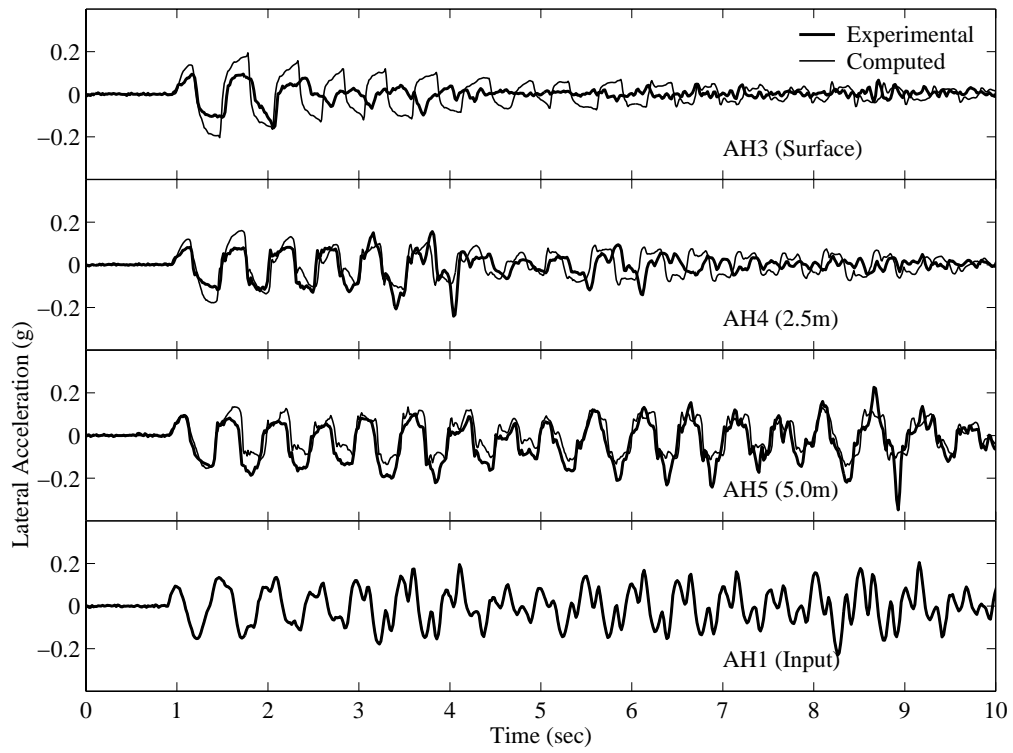


Figure 11: Model 1 recorded and computed acceleration time histories

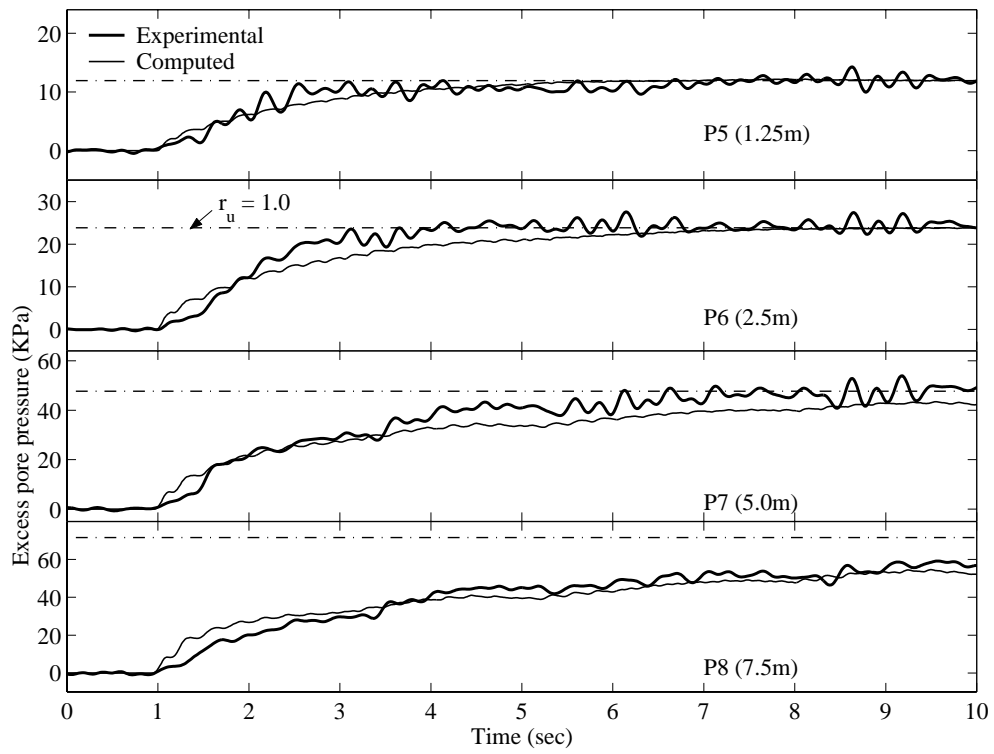


Figure 12: Model 1 recorded and computed excess pore pressure time histories

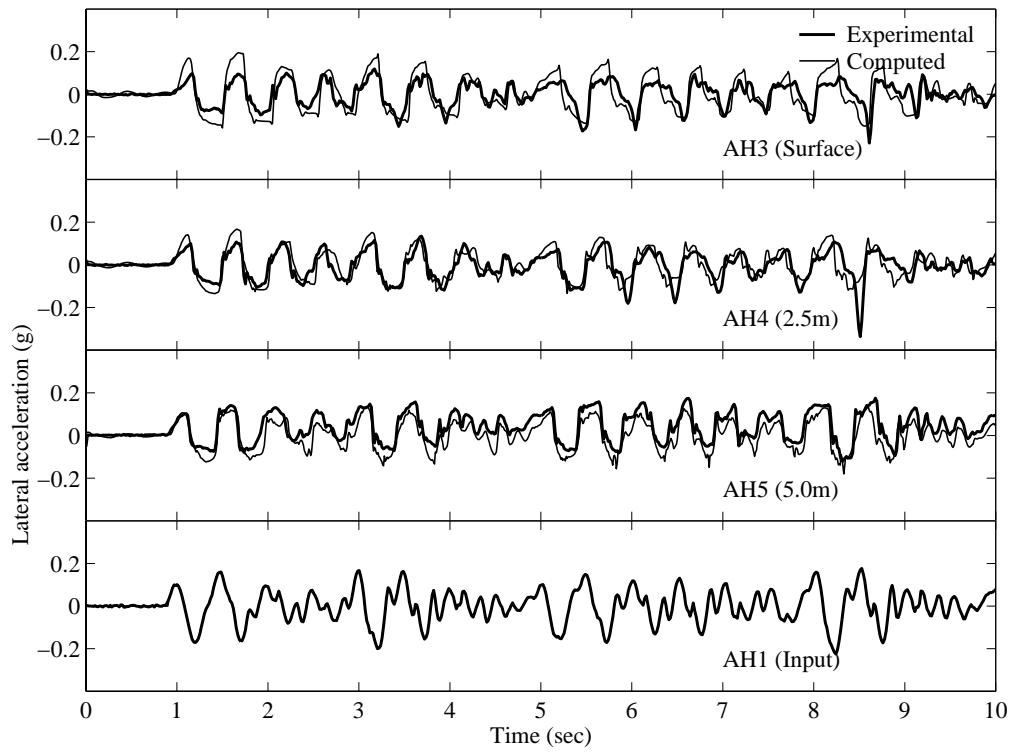


Figure 13: Model 2 recorded and computed acceleration time histories

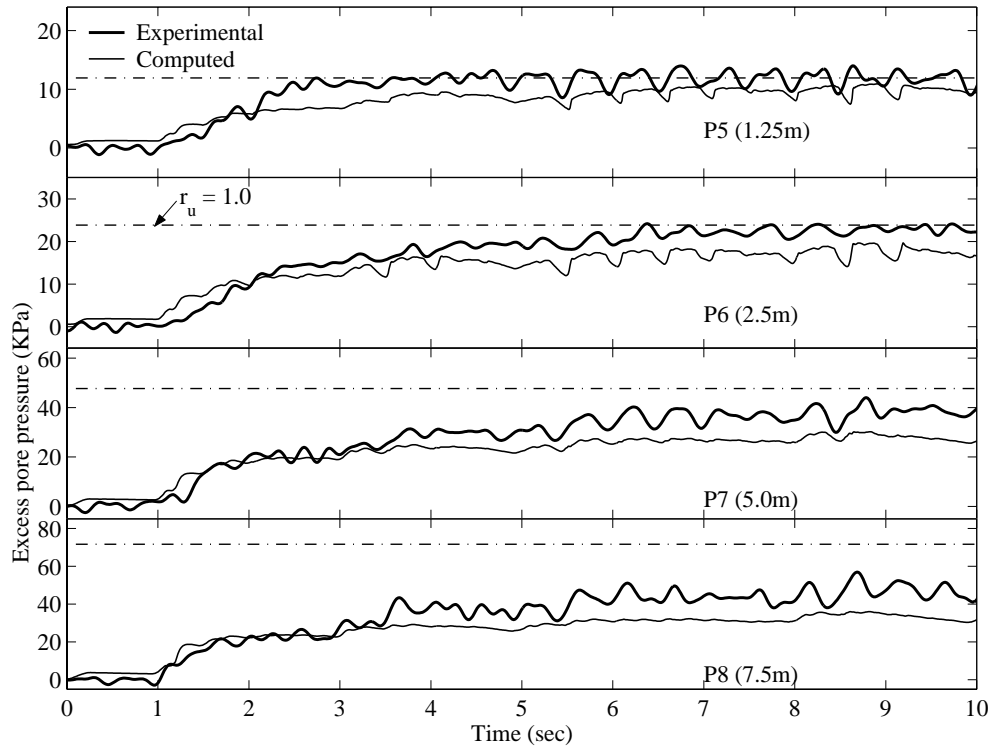


Figure 14: Model 2 recorded and computed excess pore pressure time histories



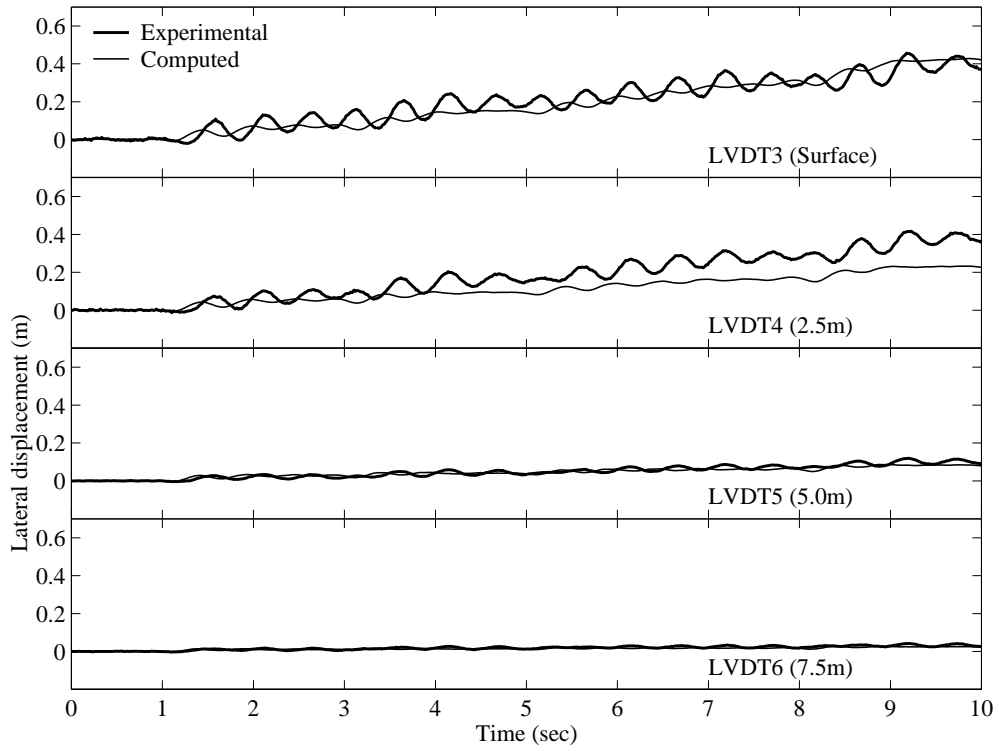


Figure 15: Model 2 recorded and computed lateral displacement histories

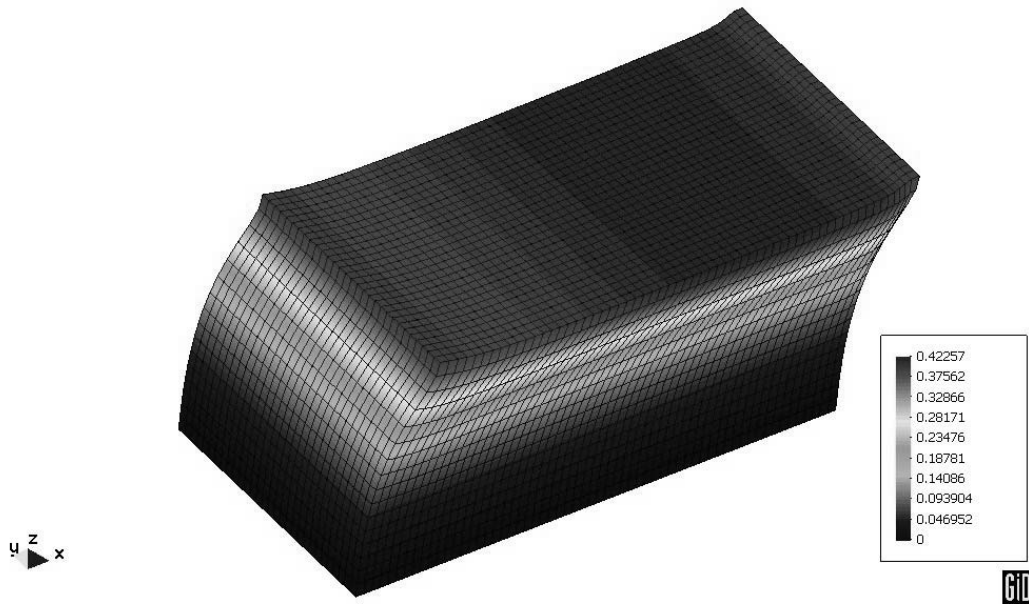


Figure 16: Deformed mesh (factor of 10) of Model 2 after 10 seconds of excitation (unit: m)

## **7. Conclusions**

This paper presents the analysis and solution strategies employed in ParCYCLIC, a parallel nonlinear finite element program for the simulation of earthquake site response and liquefaction. In ParCYCLIC, finite elements are employed within an incremental plasticity coupled solid-fluid formulation. Extensive calibration of ParCYCLIC has been conducted with results from experiments and full-scale response of earthquake simulations involving ground liquefaction.

ParCYCLIC employs the single-program-multiple-data (SPMD) paradigm, a common approach in developing application software for distributed memory parallel computers. The solution strategy in ParCYCLIC is based on the parallel row-oriented sparse solver (Mackay and Law (1993)). An automatic domain decomposer based on METIS routines (Karypis and Kumar 1997) is implemented in ParCYCLIC, in which the multilevel nested dissection algorithm is used to order the finite element nodes.

ParCYCLIC has been successfully ported on IBM SP machines, SUN super computers, and Linux workstation clusters. Large-scale experimental results for gird models and 3-D geotechnical simulations are presented to demonstrate the performance of ParCYCLIC. Excellent parallel speedups are reported from the simulation results. Furthermore, the results show that ParCYCLIC is scalable to a large number of processors. The parallel computational strategies employed in ParCYCLIC are general and can be adapted to other similar applications without difficulties.

Centrifuge tests were simulated using ParCYCLIC on a parallel computer and preliminary results are presented. It is shown that ParCYCLIC can be used to simulate large-scale problems, which would otherwise be infeasible using single-processor computers due to the limited memory.

## **Acknowledgements**

This research was supported in part by the National Science Foundation, Grant Number CMS-0084616 to University of California, San Diego, and Grant Number CMS-0084530 to Stanford University. Additional funding was also provided by the NSF cooperative agreement ACI-9619020 through computing resources provided by the National Partnership for Advanced Computational

Infrastructure at the San Diego Supercomputer Center. The authors are most grateful to Professor Ricardo Dobry (Rensselaer Polytechnic Institute) and Professor Victor Taboada (Universidad Nacional Autónoma de México) for sharing the centrifuge data (VELACS Models 1 and 2).

## References

- Adalier K, Elgamal A, Meneses J, and Baez JI. (2003). "Stone Column as Liquefaction Countermeasure in Non-plastic Silty Soils." *Soil Dynamics and Earthquake Engineering*, (accepted June 12, 2003).
- Aluru NR. (1995). "Parallel and Stabilized Finite Element Methods for the Hydrodynamic Transport Model of Semiconductor Devices," Ph.D. Thesis, Department of Civil Engineering, Stanford University.
- Arulmoli K, Muraleetharan KK, Hossain MM, and Fruth LS. (1992). "VELACS: Verification of Liquefaction Analyses by Centrifuge Studies, Laboratory Testing Program, Soil Data Report." *Report*, The Earth Technology Corporation, Project No. 90-0562, Irvine, CA.
- Bao H, Bielak J, Ghattas O, O'Hallaron DR, Kallivokas LF, Shewchuk JR, and Xu J. (1998). "Large-scale Simulation of Elastic Wave Propagation in Heterogeneous Media on Parallel Computers." *Computer Methods in Applied Mechanics and Engineering*, 152(1-2), 85-102.
- Bielak J, Xu J, and Ghattas O. (1999). "Earthquake Ground Motion and Structural Response in Alluvial Valleys." *Journal of Geotechnical and Geoenvironmental Engineering*, 125(5), 404-412.
- Bielak J, Hisada Y, Bao H, Xu J, and Ghattas O. (2000). "One- Vs Two- or Three- Dimensional Effects in Sedimentary Valleys." *12th World Conference on Earthquake Engineering*, New Zealand, Feb.
- Biot MA. (1962). "The Mechanics of Deformation and Acoustic Propagation in Porous Media." *Journal of Applied Physics*, 33(4), 1482-1498.
- Chan AHC. (1988). "A Unified Finite Element Solution to Static and Dynamic Problems in Geomechanics," Ph.D. Dissertation, University of Wales, Swansea, U.K.
- De Santiago E, and Law KH. (1996). "A Distributed Finite Element Method for Solving the Incompressible Navier-Stokes Equations." *International Journal for Numerical Methods in Engineering*, 39, 4243-4258.
- Dobry R, and Taboada VM. (1994). "Experimental Results of Model No.2 at RPI." *Proceedings of the International Conference on the Verification of Numerical Procedures for the Analysis of Soil Liquefaction Problems, Vol. 2*, Aarulanandan K, Scott RF eds., Rotterdam: Balkema, 2, 1341-1352.
- Dobry R, Taboada V, and Liu L. (1995). "Centrifuge Modeling of Liquefaction Effects During Earthquakes." *Proc. 1st Intl. Conf. On Earthquake Geotechnical Engineering, IS-Tokyo*, K. Ishihara, Balkema, Rotterdam, Tokyo, Japan, Nov. 14-16, 3, 1291-1324.

- Elgamal A, Parra E, Yang Z, and Adalier K. (2002a). "Numerical Analysis of Embankment Foundation Liquefaction Countermeasures." *Journal of Earthquake Engineering*, 6(4), 447-471.
- Elgamal A, Yang Z, and Parra E. (2002b). "Computational Modeling of Cyclic Mobility and Post-Liquefaction Site Response." *Soil Dynamics and Earthquake Engineering*, 22(4), 259-271.
- Elgamal A, Yang Z, Parra E, and Ragheb A. (2003). "Modeling of Cyclic Mobility in Saturated Cohesionless Soils." *Int. J. Plasticity*, 19(6), 883-905.
- Fenves SJ, and Law KH. (1986). "A Node-Addition Model for Symbolic Factorization." *ACM Transaction on Mathematical Software*, 12(1), 37-50.
- Golub GH, and Van Loan CF. (1989). *Matrix Computations*, The Johns Hopkins University Press, Baltimore and London.
- Herndon B, Aluru N, Raefsky A, Goossens RJG, Law KH, and Dutton RW. (1995a). "A Methodology for Parallelizing PDE Solvers: Applications to Semiconductor Device Simulation." *Seventh SIAM Conference on Parallel Processing for Scientific Computing*, SIAM, San Francisco, CA.
- Herndon B, Aluru N, Raefsky A, Goossens RJG, Law KH, and Dutton RW. (1995b). "A Methodology for Parallelizing PDE Solvers: Applications to Semiconductor Device Simulation." *the Seventh SIAM Conference on Parallel Processing for Scientific Computing*, San Francisco, CA.
- Hisada Y, Bao H, Bielak J, Ghattas O, and O'Hallaron DR. (1998). "Simulations of Long-period Ground Motions During the 1995 Hyogoken-Nanbu (Kobe) Earthquake Using 3D Finite Element Method." *Proceedings of the 2nd International Symposium on Effect of Surface Geology on Seismic Motion*, Yokohama, Japan, December, 59-66.
- Ishihara K, Tatsuoka F, and Yasuda S. (1975). "Undrained Deformation and Liquefaction of Sand under Cyclic Stresses." *Soils and Foundations*, 15(1), 29-44.
- Karypis G, and Kumar V. (1997). *METIS, a Software Package for Partitioning Unstructured Graphs, Partitioning Meshes and Compute Fill-Reducing Ordering of Sparse Matrices*, Technical Report, Department of Computer Science, University of Minnesota.
- Krysl P, and Belytschko T. (1998). "Objected-oriented Parallelization of Explicit Structural Dynamics with PVM." *Computers and Structures*, 66, 259-273.
- Krysl P, and Bittnar Z. (2001). "Parallel Explicit Finite Element Solid Dynamics with Domain Decomposition and Message Passing: Dual Partitioning Scalability." *Computers and Structures*, 79, 345-360.
- Lacy S. (1986). "Numerical Procedures for Nonlinear Transient Analysis of Two-phase Soil System," Ph.D. Thesis, Princeton University, NJ, U.S.A.
- Law KH. (1981). "Graph-Theoretic Approaches to Structural Analysis," Ph.D. Thesis, Department of Civil Engineering, Carnegie-Mellon University.
- Law KH, and Mackay DR. (1993). "A Parallel Row-oriented Sparse Solution Method for Finite Element Structural Analysis." *International Journal for Numerical Methods in Engineering*, 36, 2895-2919.

- Law KH. (1994). "Large Scale Engineering Computations on Distributed Memory Parallel Computers and Distributed Workstations." *NSF Workshop on Scientific Supercomputing, Visualization and Animation in Geotechnical Earthquake Engineering and Engineering Seismology*, Carnegie-Mellon University, October.
- Liu JWH. (1986). "A Compact Row Storage Scheme for Cholesky Factors using Elimination Tree." *ACM TOMS*, 12, 127.
- Liu JWH. (1988). "A Generalized Envelope Method for Sparse Factorization by Rows." *Technical Report CS-88-09*, Department of Computer Science, York University, Canada.
- Mackay DR, Raefsky A, and Law KH. (1991). "An Implementation of A Generalized Sparse/Profile Finite Element Solution Method." *Computer and Structure*, 41(4), 723-737.
- Mackay DR. (1992). "Solution Methods for Static and Dynamic Structural Analysis on Distributed Memory Computers," Ph.D. Thesis, Department of Civil Engineering, Stanford University.
- McKenna F. (1997). "Object Oriented Finite Element Analysis: Frameworks for Analysis Algorithms and Parallel Computing," PhD Thesis, Department of Civil Engineering, University of California, Berkeley.
- Mroz Z. (1967). "On the Description of Anisotropic Work Hardening." *J. Mechanics and Physics of Solids*, 15, 163-175.
- Nikishkov GP, Kawka M, Makinouchi A, Yagawa G, and Yoshimura S. (1998). "Porting an Industrial Sheet Metal Forming Code to a Distributed Memory Parallel Computer." *Computers and Structures*, 67, 439-449.
- NPACI. (2003). *Blue Horizon User Guide*, <http://www.npaci.edu/BlueHorizon/>, San Diego, CA.
- Parra E. (1996). "Numerical Modeling of Liquefaction and Lateral Ground Deformation Including Cyclic Mobility and Dilation Response in Soil Systems," Ph.D. Thesis, Dept. of Civil Engineering, Rensselaer Polytechnic Institute, Troy, NY.
- Parra E, Adalier K, Elgamal A-W, Zeghal M, and Ragheb A. (1996). "Analyses and Modeling of Site Liquefaction Using Centrifuge Tests." *Eleventh World Conference on Earthquake Engineering*, Acapulco, Mexico, June 23-28.
- Prevost JH. (1985). "A Simple Plasticity Theory for Frictional Cohesionless Soils." *Soil Dynamics and Earthquake Engineering*, 4(1), 9-17.
- Romero ML, Miguel PF, and Cano JJ. (2002). "A Parallel Procedure for Nonlinear Analysis of Reinforced Concrete Three-dimensional Frames." *Computers and Structures*, 80, 1337-1350.
- Schreiber R. (1982). "A New Implementation of Sparse Gaussian Elimination." *ACM TOMS*, 8, 256.
- Suarjana M. (1994). "Conjugate Gradient Method for Linear and Nonlinear Structural Analysis on Sequential and Parallel Computers," Ph.D. Thesis, Department of Civil Engineering, Stanford University.
- Taboada VM. (1995). "Centrifuge Modeling of Earthquake-Induced Lateral Spreading in Sand Using a Laminar Box," Ph.D. Thesis, Rensselaer Polytechnic Institute, Troy, NY.

- Tan TS, and Scott RF. (1985). "Centrifuge Scaling Considerations for Fluid-Particle Systems." *Geotechnique*, 35(4), 461-470.
- Yang Z. (2000). "Numerical Modeling of Earthquake Site Response Including Dilation and Liquefaction," Ph.D. Thesis, Dept. of Civil Engineering and Engineering Mechanics, Columbia University, New York, NY.
- Yang Z, and Elgamal A. (2002). "Influence of Permeability on Liquefaction-Induced Shear Deformation." *J. Engineering Mechanics*, 128(7), 720-729, ASCE.
- Yang Z, Elgamal A, and Parra E. (2003). "A Computational Model for Cyclic Mobility and Associated Shear Deformation." *Journal of Geotechnical and Geoenvironmental Engineering, ASCE*, (accepted).
- Zienkiewicz OC, Chan AHC, Pastor M, Paul DK, and Shiomi T. (1990). "Static and Dynamic Behavior of Soils: A Rational Approach to Quantitative Solutions: I. Fully Saturated Problems." *Proceedings of the Royal Society London, Series A, Mathematical and Physical Sciences*, 429, 285-309.